Electronic Supplementary Information

Molecularly Thin Organic Single-Crystalline p-n Heterojunctions by Interfacial Heteroepitaxy for High-Performance Polarization-Sensitive Photodetectors

Ximeng Yao,[‡a] Xianfeng Shen,[‡a] Xinzi Tian,[‡a,b] ,Yali Yu,[c,d] Jiarong Yao,[a,e] Yanling Xiao,[f] Jiansheng Jie,[f] Zhongming Wei,[*c,d] Rongjin Li[*a] and Wenping Hu[a]

[a.] Key Laboratory of Organic Integrated Circuits, Ministry of Education & Tianjin Key Laboratory of Molecular Optoelectronic Sciences, Department of Chemistry, School of Science, Tianjin University, Tianjin 300072, China. E-mail: lirj@tju.edu.cn

[b.] China Fire and Rescue Institute, Beijing 102202, China.

[c.] State Key Laboratory of Semiconductor Physics and Chip Technologies, Institute of Semiconductors, Chinese Academy of Sciences, Beijing 100083, China. E-mail: zmwei@semi.ac.cn.

[d.] Center of Materials Science and Optoelectronics Engineering, University of Chinese Academy of Sciences, Beijing 100049, China.

[e.] Engineering Research Center of Coal-Based Ecological Carbon Sequestration Technology of the Ministry of Education, Shanxi Datong University, Datong, Shanxi Province 037009, China.

[f.] Institute of Functional Nano & Soft Materials (FUNSOM), Jiangsu Key Laboratory for Carbon-Based Functional Materials & Devices, Soochow University, Suzhou 215123, China.

Contents

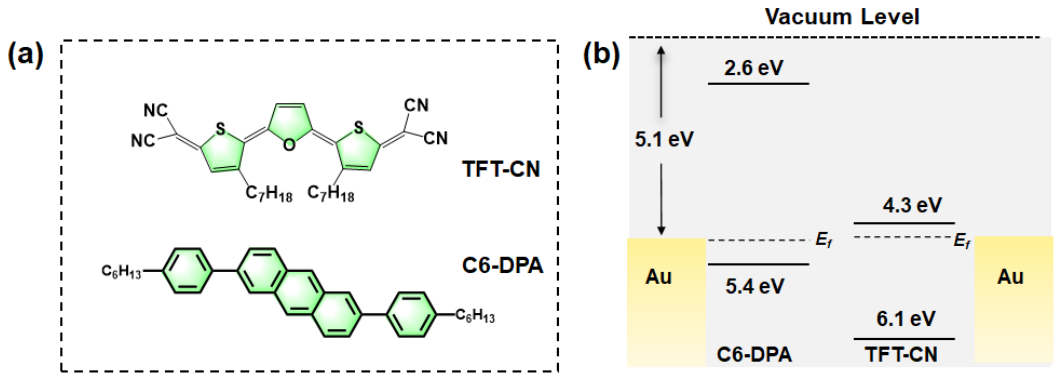

Fig. S1 (a) Chemical structures of C6-DPA and TFT-CN. (b) Energy level diagrams of C6-DPA and TFT-CN.

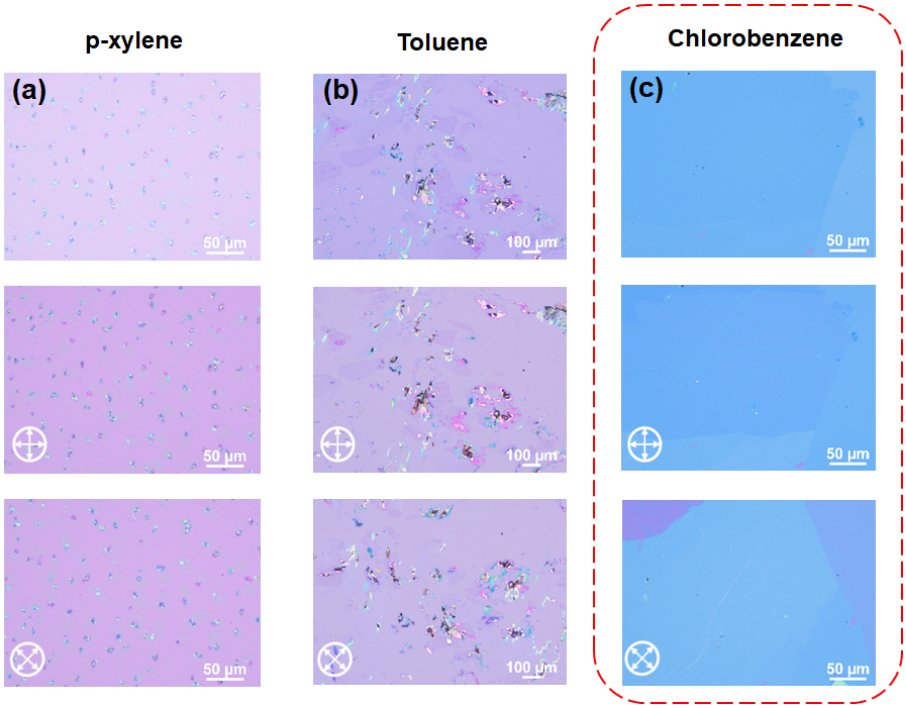

Fig. S2 Optical microscopy images and corresponding polarized optical microscopy images of heterojunctions grown in different solvents. (a) p-Xylene, (b) Toluene, (c) Chlorobenzene.

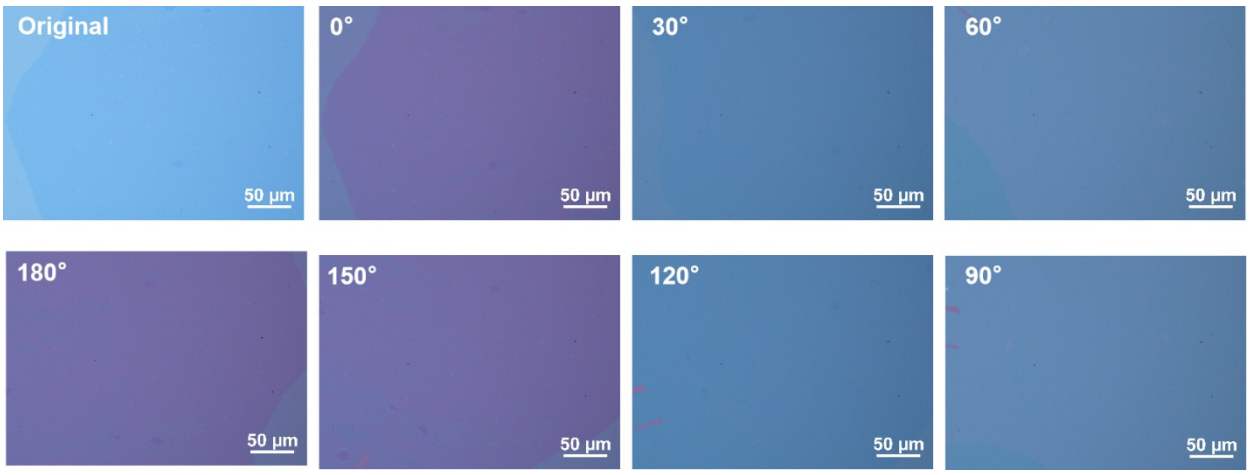

Fig. S3 Polarized optical microscopy (POM) images of molecularly thin single-crystalline p-n heterojunctions composed of 2D molecular crystals (2DMCs), shown at different angles.

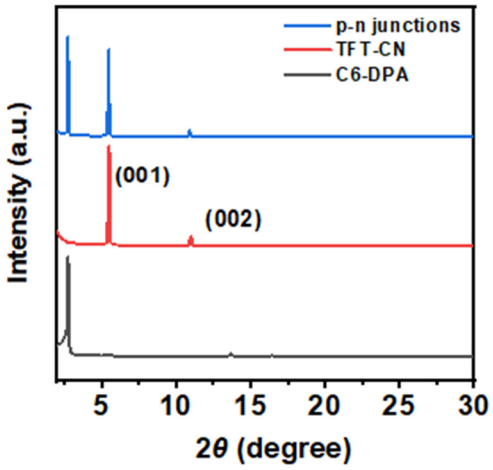

Fig. S4 X-ray diffraction (XRD) patterns of the 2D molecular crystals (2DMCs) of C6-DPA, TFT-CN, and their p-n heterojunctions.

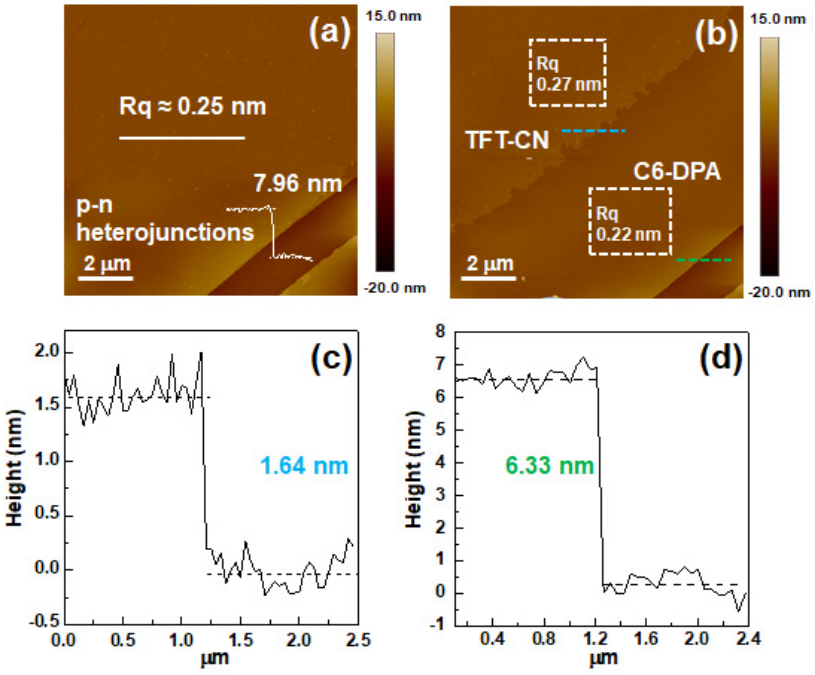

Fig. S5 (a-b) AFM images of C6-DPA, TFT-CN, and their p-n heterojunctions. (c-d) Height profiles of TFT-CN and C6-DPA within the p-n heterojunctions.

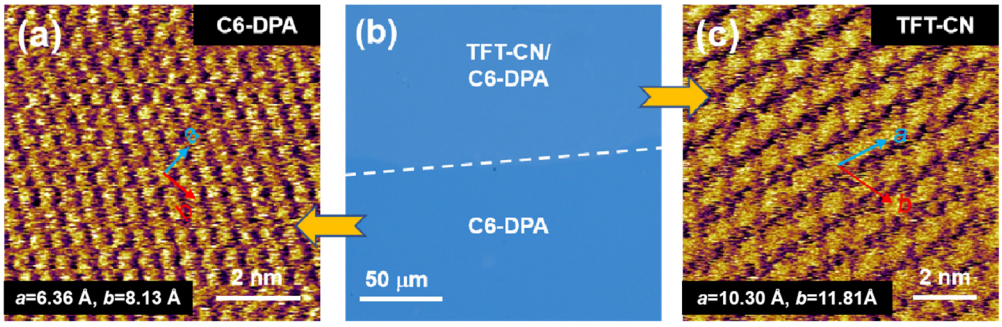

Fig. S6 Additional high-resolution AFM (HR-AFM) images of TFT-CN and C6-DPA at different locations within the p-n heterojunctions. The lattice parameters are 3b (C6-DPA) = 24.39 Å and 2b (TFT-CN) = 23.62 Å, corresponding to a lattice mismatch ratio of approximately 3.2%.

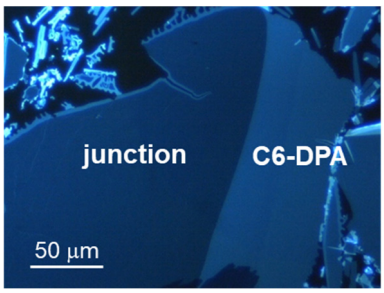

Fig. S7 Photoluminescence (PL) image of C6-DPA (right) and the heterojunction (left).

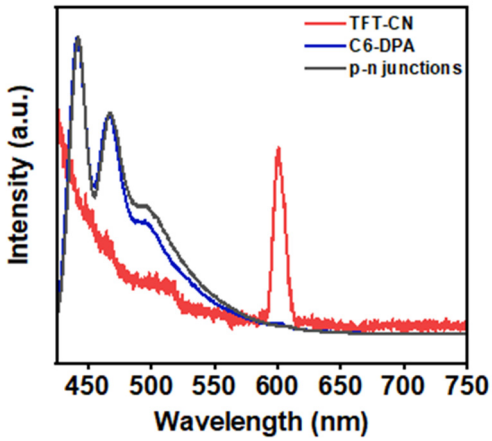

Fig. S8 PL spectra of the heterojunctions and its individual components 2DMC.

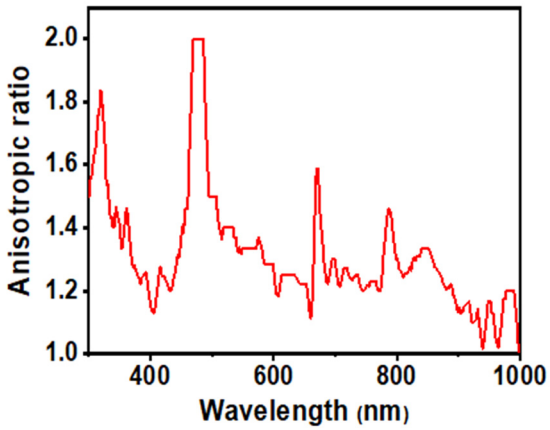

Fig. S9 Anisotropic absorption ratios at the measured wavelengths.

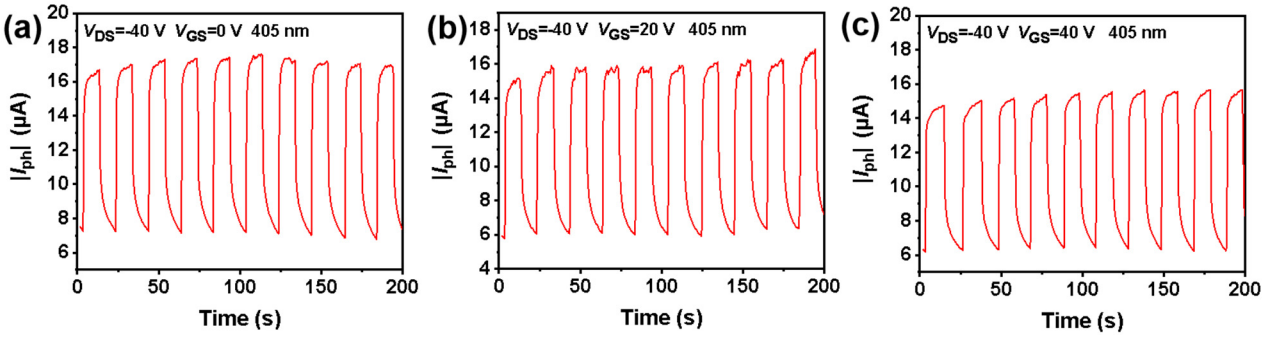

Fig. S10 Photo-switching at different gate voltages.

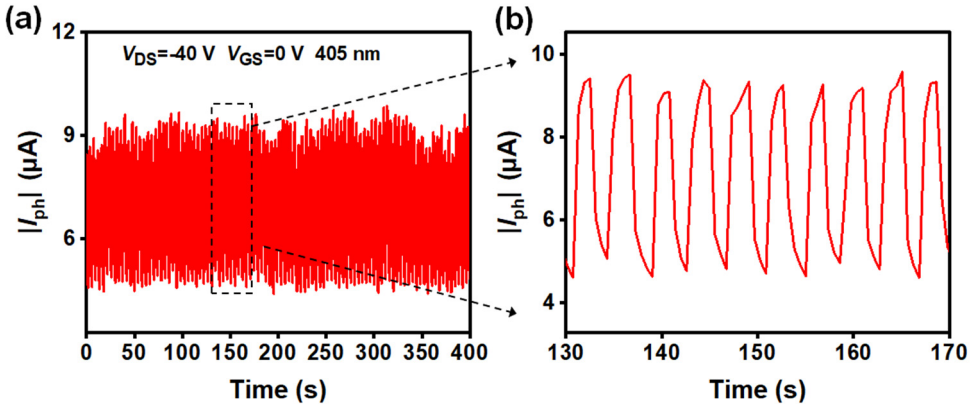

Fig. S11 (a) Switching stability of p-n heterojunctions under a pulsed 405 nm laser at a drain bias of -40 V. (b) An enlarged view of 10 switching cycles from (a).

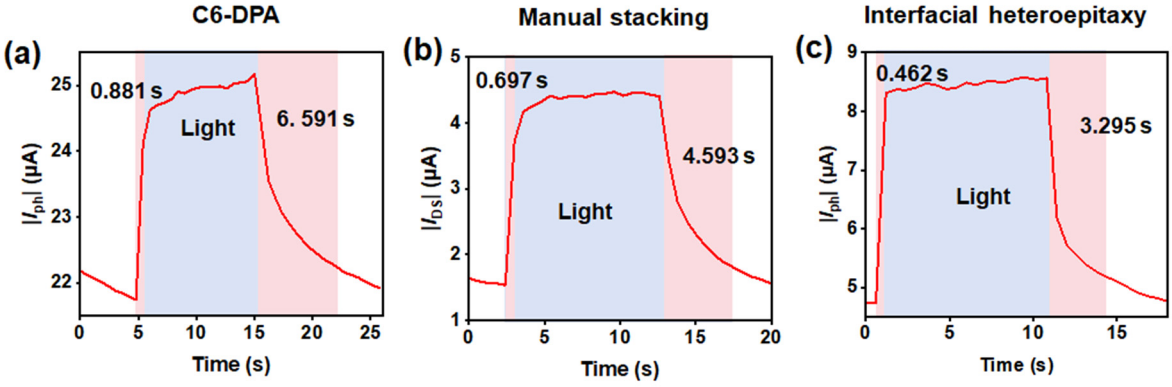

Fig. S12 Photo-switching curves showing rise and decay processes for (a) C6-DPA 2DMC, (b) manually stacked p-n heterojunctions, and (c) interfacial heteroepitaxial p-n heterojunctions.

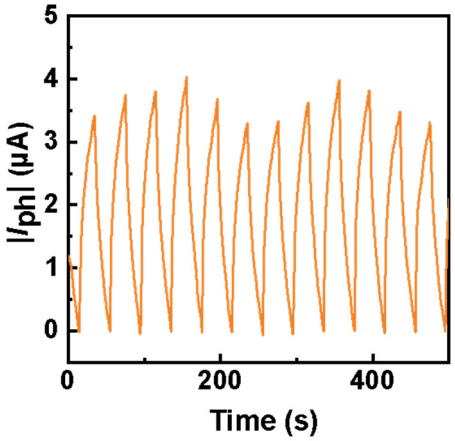

Fig. S13 Current-time curve of manually stacked heterojunctions under periodic polarization direction changes of 405 nm light. The polarization ratio (PR) is 1.3 at 405 nm, while no significant PR is observed at 808 nm.

Table S1 Summary of figures of merit for reported linearly polarized photodetectors based on organic semiconductors[1-8].

Materials	Wavelength (nm)	R (A W^{-1})	D^* (Jones)	PR	Methods	Refs.
DPA	450	N/A	N/A	1.9	PVT	[1]
DTT-8	365	3.58×10^4	N/A	3.15	epitaxy	[2]
C8-BTBT	254	0.34	N/A	2.26	blade coating	[3]
TIPS-pentacene	532	0.0015	N/A	1.42	writing	[4]
CuPc	785	200	N/A	1.4	PVT	[5]
Ph-BTBT-C10	365	1.47×10^4	N/A	3.85	epitaxy	[6]
Alq_3 MWCs	365	1234	8.7×10^{13}	2.1	microchannel	[7]
BPTTE	360	377.9	9.8×10^{10}	2.73	PVT	[8]
C6-DPA/TFT-CN	365-808	942	1.08×10^{14}	2.4	epitaxy	This Work

References:

1 T. Wang, K. Zhao, P. Wang, W. Shen, H. Gao, Z. Qin, Y. Wang, C. Li, H. Deng, C. Hu, L. Jiang,

H. Dong, Z. Wei, L. Li and W. Hu, *Adv. Mater.*, 2022, **34**, 2105665.

2 Y. Zhang, S. Yang, W. Wang, S. Zhang, Z. Wang, Z. Niu, Y. Guo, G. Li, R. Li and W. Hu, *ACS Appl. Mater. Interfaces,* 2024, **16**, 23634.

3 S. Chen, Z. Liu, H. Long, J. Yang, Z. Li, Z. Cai, Z. Qu, L. Shao, X. Shi, L. Jiang, W. Xu, H. Dong, Z. Wei, Y. Qiao and Y. Song, *Adv. Funct. Mater.*, 2023, **33**, 2212158.

4 S. Chen, X. Ma, Z. Cai, H. Long, X. Wang, Z. Li, Z. Qu, F. Zhang, Y. Qiao and Y. Song, *Adv. Mater.*, 2022, **34**, 2200928.

5 M. Li, Q. Du, Y. Zhang, Y. Liu, W. Wang, F. Wang and S. Qin, *J. Mater. Chem. C*, 2023, **11**, 14456-14463.

6 M. Dong, Y. Zhang, J. Zhu, X. Zhu, J. Zhao, Q. Zhao, L. Sun, Y. Sun, F. Yang and W. Hu, *Adv. Mater.*, 2024, **36**, 2409550.

7 S.-X. Li, Y. An, X.-C. Sun, H. Zhu, H. Xia and H.-B. Sun, *Sci. China Mater.*, 2022, **65**, 3105-3114.

8 Y. Zhang, Z. Qin, H. Gao, T. Wang, C. Gao, X. Zhang, W. Hu and H. Dong, *Adv. Mater.*, 2024, **36**, 2404309.